Investigation of Polarization Dependent Gain Dynamics in a Bulk SOA

B.F. Kennedy [a], S. Philippe [b], F. Surre [a], A.L. Bradley [b], D. A. Reid [a] and P. Landais [a]

[a]Research Institute for Networks and Communications Engineering, Radio and Optical communications, Dublin City University,Ireland.
[b]School of Physics, Trinity College Dublin, Ireland.

1 Introduction

All-optical signal processing techniques using Semiconductor Optical Amplifiers (SOAs) such as Cross-Gain Modulation (XGM), Cross-Phase Modulation (XPM) and Four-Wave Mixing (FWM) continue to be developed [1]. The anticipated growth in demand for bandwidth leads to the development of these systems at ever increasing data rates. This means that the gain of the SOA is modulated on smaller and smaller timescales. It has been demonstrated that the ultra-fast gain processes are dominant for pulsewidths below 10 ps [2]. The level of polarization dependence introduced by these ultra-fast gain process has been treated theoretically on sub-picosecond pulses [3] and [4]. However it has not been demonstrated or investigated for picosecond pulses. This is the purpose of our paper to study the polarization dependence of ultra-fast gain process in SOA. This polarization dependence, if exits must impact on the operation of optical systems through.
The results presented in this paper quantifies the effects of the polarization dependence of several gain processes; the carrier density pulsations (CDP) and carrier heating (CH) processes using two experimental setups. The first experiment is based four-wave-mixing generated in the SOA. A variation in the detuning between pump and probe signals injected into the device allows the gain to be modulated at different frequencies. It is then possible to fit this experimental data to

a theoretical expression in order to retrieve the carrier recovery time and linewidth enhancement factors (LEF). Once several considerations, detailed later are taken into account it is possible to obtain polarization resolved results by varying the polarization of the injected pump and probe signals. In the second experiment, the polarization dependent of 2 ps pulses propagating in an SOA is investigated, using the Frequency Resolved Optical Gating (FROG) technique. FROG may be described as a spectrally resolved autocorrelation. This technique allows for a complete characterization of the pulses, in both the temporal and spectral domains. The pulses are amplified through the SOA in both the unsaturated and saturated regimes, and the polarization dependence is measured in each case.

This paper is organized as follows: In Section 2 the FWM setup and results are presented, in Section 3 the FROG experiment and results are detailed, in Section 4 a comparison between the results achieved with these experiment is given with an interpretation, and finally in Section 5 conclusions are presented and drawn. In both experiments, the SOA under test is commercially available under reference A1901. It is a 300 μm tensile strained InGaAsP bulk active waveguide, terminated by 150 μm lateral tapered active regions. It is biased at 200 mA and temperature controlled at 23^oC. **Its gain peak is at 1515 nm and with a fibre-to-fibre gain given at 24 dB at 200 mA.**

2 FWM Experiment

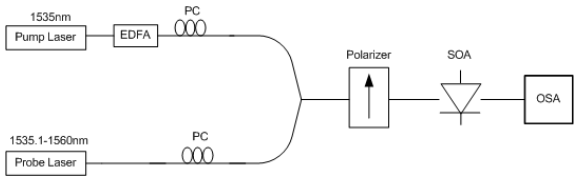

Fig. 1. Experimental setup for the FWM experiment

Two signals called the pump and the probe at frequency f_p and f_s, respectively are launched into a semiconductor optical amplifier. Due to the third order non-linear effect of the semiconductor material, these signal beat together generating a modulation of the complex refractive index of the waveguide at the frequency detuning $\Omega = |f_s - f_p|$.

This lead to a generation of waves separated spectrally by Ω. Five FWM processes are contributing to this wave generation, CDP which is an interband effect, CH, spectral-hole-burning (SHB), two-photon absorption (TPA), and Kerr effect which are intraband effects. The first three processes are stronger than the last two for Ω less than 8 THz, thus within the experimental conditions. For smaller values of Ω, CDP is the most efficient effect. As Ω increases, the efficiency of CDP reduces and then CDP cannot fellow the modulation. CH starts to be the most efficient effect and then SHB. Increasing Ω makes possible the observation of the contribution of each of the nonlinear gain processes produced by CDP and CH [5] - [9]. This technique has never been used to measure the polarization dependence of CDP and CH, we propose to do it if some considerations are taken into account.

Two external cavity tunable CW lasers are used to perform the FWM experiment as depicted in Fig.1. The wavelength of the pump is 1535 nm, which is within the 3 dB gain bandwidth of the device. The wavelength of the probe is varied from 1535 nm to 1560 nm in steps as low as 0.1 nm. Ideally it would be preferable to have the pump wavelength closer to the gain peak of the device, which occurs at 1515 nm, but there is a restriction due to the EDFA which does not amplify the signal significantly, below 1535 nm. The EDFA is required to amplify the pump signal, as a strong intensity is necessary in order to suppress the gain of the device. The choice of wavelengths used for the pump and the probe thus involves a trade-off between the gain spectrum of the EDFA, which operates in the C-band, and the gain spectrum of the SOA, respectively. In this experiment with the frequency detunnig available, measurements of time-varying phenomena recovering on timescales greater than 300 fs is achieved. The pump power is maintained at 9 dBm for all measurements, whilst the probe power is constant at -4 dBm. A difference of 13 dB between the powers of the pump and the probe is set to produce the maximum value for the conversion efficiency [9], given by:

$$\rho_{exp} = \frac{P_{conj}}{P_{probe}}, \tag{1}$$

where P_{conj} is the power of the symmetric signal of the probe with respect to the pump signal, and P_{probe} the probe power. Both powers are measured at the SOA output. An optical spectrum anaylser (OSA) with a resolution bandwidth of 0.07 nm is used to measure these output powers. The polarization of both the pump and the probe is controlled using a polarizer and a polarization controller (PC). The polarizer ensures that: i) both signals are linearly polarized, ii) they are co-polarized, a requirement for efficient FWM, and iii) they are injected along the same axis of the PM lensed fibre. The angle, θ between the co-polarized pump and probe signals and the TE axis of SOA is varied with respect to the axis of the device by physically rotating the PM lensed fibre. The coupling from the lensed fibre to the SOA is maintained at a constant level as the polarization is varied and in both arms PCs are used to align signals along the axis of polarizer to keep constant probe and pump powers. The conversion efficiency is recorded as a function of wavelength detuning between the pump and the probe for a given value of θ.
The conversion efficiency can be expressed theoretically as follows:

$$\rho_{th} = S_0^2(L)|f_{cdp}(\Omega) + f_{ch}(\Omega)|^2 \tag{2}$$

where S_0 represents the pump photon density and the contributions from carrier density pulsations (f_{cdp}) and carrier heating (f_{ch}) are defined as follows [16]:

$$f_{cdp}(\Omega) = -\frac{1}{S_{sat}}\frac{1 - j\alpha_{cdp}}{2(1 - j2\pi\Omega\tau_{cdp})} \tag{3}$$

$$f_{ch}(\Omega) = -\frac{1}{S_{ch}}\frac{1 - j\alpha_{ch}}{(1 - j2\pi\Omega\tau_{ch})(1 - j2\pi\Omega\tau_{shb})} \tag{4}$$

where the α_i parameters refer to the linewidth enhance factors, the τ_i parameters refer to the carrier recovery times and the S_i parameters refer to the characteristic power associated with each process. By fitting the efficiency data it is possible to retrieve the above parameters related to CDP and CH as a function of the angle of θ. However several considerations must be taken into account. Firstly, the polarization dependence of SHB cannot be determined using our experiment. The experiment is limited on purpose to detuning of less than

3.5 THz, corresponding to a time resolution of approximately 300 fs, larger than the characteristic time of SHB. Above this detuning, a polarization dependence of the efficiency will occur, which will deteriorate the precision of our measurements [10]. Secondly, the spectral dependence of the gain can be neglected [11]. For Ω range of less than 3.5 THz the gain varies by less than 1 dB. Thirdly, the value for S_0 is also fixed as the pump signal is maintained at a constant power for all measurements.
The next step involves using a minimization technique in order to minimize the error between the experimental efficiency data and the theoretical efficiency, defined in Eqns. (3)-(4). The parameters in these equations are given initial values and six of these parameters are set as variables in order to reduce the error between the experimental and theoretical efficiency. This fitting is performed as a function of angular frequency detuning for the following parameters: S_{sat}, α_{cdp}, τ_{cdp}, S_{ch}, α_{ch} and τ_{ch}.

The experimental efficiency and the fitted efficiency are plotted as a function of Ω in Fig. 2 for θ of 30^o, together with the calculated contribution from CDP and CH. The accuracy of the fitting can be seen on the graph. For a small frequency detuning CDP has the largest effect on the efficiency, as expected. CDP decreases by approximately 20 dB/decade, and CH becomes more important as Ω is increased.

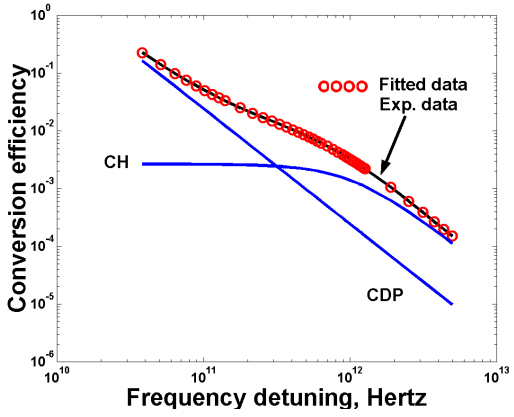

Fig. 2. Experimental data (o) and fitted curves for CDP and CH processes at $\theta = 30^o$

The fitting is performed for a range of injection polarizations between -30^o and 90^o. The accuracy of the fitting may be gauged by consid-

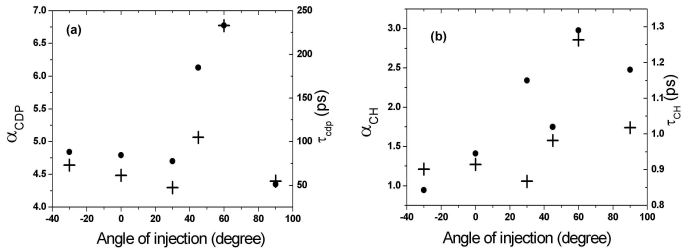

Fig. 3. Linewidth enhancement factor(•) and recovery time (+) obtained from FWM experiment for both (a) CDP and (b) CH.

ering the variance between the experimental data and the fitted data. The variance calculated for each angle of polarization is less than 0.001%. Fig. 3(a) shows the extracted values for the LEF, α_{cdp}, and the carrier recovery time, τ_{cdp}, associated with CDP as a function of the polarization angle. α_{cdp} varies from a value of less than 4.5 at 30^o up to a peak of 6.5 at 60^o. Similarly the carrier recovery time varies from 50 ps to 230 ps, for the same values of θ.

Fig. 3(b) shows the LEF, α_{ch}, and the recovery time, τ_{ch}, associated with CH, as a function of injection angle. α_{ch} is approximately 1 at -30^o and peaks at 60^o with a value of almost 3.

3 FROG Experiment

In order to assess the results achieved with the FWM setup, an experiment based on the frequency resolved optical gate (FROG) is proposed to analyze pulse propagation through the SOA as a function of θ. With the FROG it is possible to observe variations of the signal intensity and the instantaneous frequency i.e. chirp as the pulse propagates through the SOA. The chirp introduced by the SOA is found experimentally by subtracting the overall chirp from the initial chirp of the source pulse [12]. In this setup shown in Fig. 4, 2 ps pulses are generated from a passively mode-locked laser, centered at 1540 nm, with a repetition rate of 10 GHz. The choice of 2 ps pulses is driven by the previous results. With 2 ps pulses it is possible to observe nonlinear gain effects dominated by CH [2]. The peak power of the pulses is 30 mW, corresponding to a pulse energy of approximately 60 fJ

and an average power of 600 μW. The pulses are injected into the SOA using the same care than in the FWM setup. A CW laser is also injected into the SOA in co-propagation at a wavelength of 1538 nm, only 2 nm from the signal wavelength. The purpose of this signal is to deplete carriers in the device in order to observe the polarization dependence of the pulses in the nonlinear gain regime of the SOA. This signal is also polarized along the axis of the PM lensed fibre and a PC is placed in the CW arm in order to control its intensity. A 1.75 nm full-width at half maximum Band-Pass Filter (BPF), centered at 1540 nm, removes the amplified CW signal at the output of the device. It would also be possible to deplete carriers in the device by amplifying the pulses using an EDFA. However, for the pulses generated in this experiment significant temporal and spectral broadening are induced from standard EDFAs, due to the long length of the doped fibre. An EDFA is used prior to injection into the FROG. It differs from the standard device in that it was specifically designed for the amplification of pulses in the order of 2 ps. The error between the experimental data and the data measured using the FROG retrieval program is below ≈ 0.007, indicating accurate measurement [13]. The temporal and spectral resolution of the FROG device used in this experiment is 100 fs and 0.1 nm at 1550 nm, respectively.

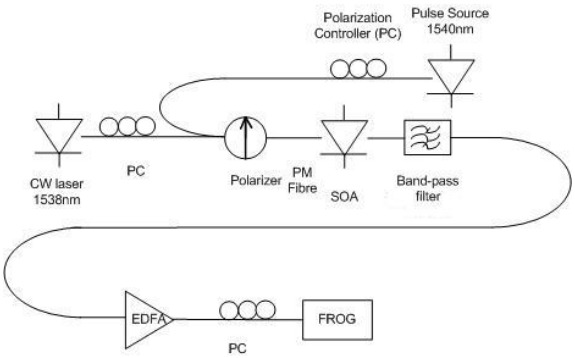

Fig. 4. Experimental setup used to determine the polarization dependence of 2 ps pulses propagating through the SOA

Fig. 5 shows the intensity and the chirp of the amplified pulses as a function of θ in the case of no CW injection. For clarity, figure represent only three angles of polarization. It can be seen that there is no significant variation in the temporal response. The pulse width remains at 2ps. The time evolution of chirp is shown in Fig 5(b). The

amplification process reduces the carrier number, leading to an increase of the effective refractive index of the active layer. This is the self-phase modulation (SPM). In the case of no CW injection negligible polarization dependence of the chirp is measured. For the pulse energy considered in this experiment, i.e. 60 fJ, the device is still operating in the linear regime well below the saturation energy in the pJ range according to the manufacturer.

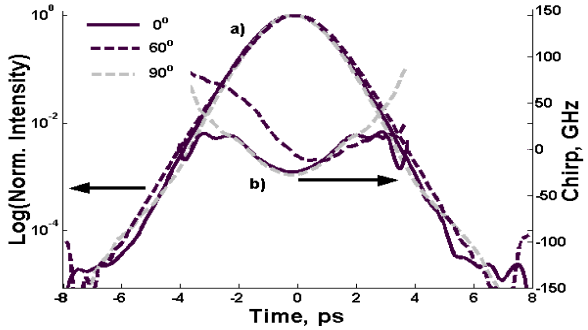

Fig. 5. Temporal and spectral FROG results for the case of no CW injection.

A 1 mW CW signal is then injected into the device. The 3 dB gain saturation occurs for an input power of 315 μW. The intensity and chirp at the output of the device can be seen in Fig. 6. In the temporal domain large pedestals are visible on both the rising and falling edges of the pulse. It has been reported that the pedestals exist on the original pulses injected into the SOA due to the presence of a saturable absorber in the mode-locked laser. The reason they are not obvious in Fig. 5 is that the amplitude of the pedestals is below the noise level. The pedestals become more significant after propagation through the SOA with CW injection, due to gain saturation in the device. This causes the pedestal present on the rising edge of the injected pulse to receive a much larger gain with respect to the center and falling edge of the pulse, thus it becomes much more pronounced. In this case the pedestal is located only approx. 17 dB from the peak of the pulse for an angle of 60^o.

There is also a pedestal present on the falling edge of the pulse. It occurs approximately 4 ps after the peak of the pulse, by which time the gain has started to recover. The gain has not, however, fully recovered from the suppression caused by the pulse, as can be seen

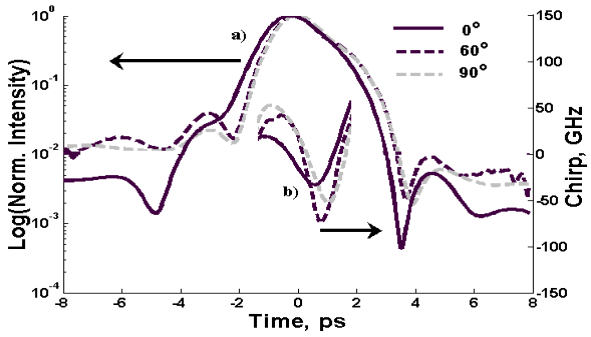

Fig. 6. Temporal and spectral FROG results for the case of 1 mW CW injection.

from the fact that the pedestal on the falling edge does not receive as much amplification as the pedestal on the rising edge, with a difference of 3 dB between rising and falling edge pedestals visible at 60^0. A variation in the amplitude of the pedestals of approximately 2 dB can be observed between angles of 60^o and 90^o. **This indicates that there is a variation in the suppression of the gain as a function of polarization for 2 ps pulses. As the ultra-fast gain processes are dominant for pulses of length 2 ps [2], the results show a polarization dependence in the saturation of the gain due to these ultra-fast processes**. This is confirmed with the chirp profile in Fig. 6 (b). A larger negative frequency components is introduced due to an increase of the non-linearities due to the gain suppression controlled by the CW signal.

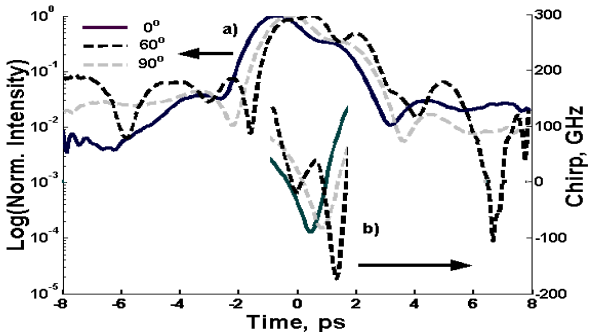

Fig. 7. Temporal and spectral FROG results for the case of 4 mW CW injection.

The CW signal is then injected into the SOA at an intensity of 4 mW, to an even larger levels of suppression. The results are shown in Fig. 7. For an injection angle of 60^o, a large number of ripples are introduced in the temporal domain. It is believed that these ripples

	0 mW CW	1 mW CW	4 mW CW
Angle	ΔChirp amp.(GHz)	ΔChirp Amp.(GHz)	ΔChirp. Amp(GHz)
0^o	11	69	182
30^o	17	64	168
45^o	19	131	182
60^o	21	132	311
90^o	14	109	207

Table 1
Chirp amplitude introduced by the SOA when no CW signal is injected and when 4 mW CW signal is injected.

originate from a beating between the pulses and the CW signal, which may occur for large levels of CW power. The pulse pedestal observed in Fig. 6 is also visible in Fig. 7 on the rising edge of the pulses. The increased gain suppression results in the pedestal being located only 12 dB from the peak of the pulse at 60^o. This result indicates the continued suppression of the gain for increasing levels of CW power. Furthermore, an increase in the polarization dependence of the gain suppression is also measured with over 4 dB variation in the amplitude of the pedestals between 0^o and 60^o. This in turn leads to an increase in the polarization dependence of the chirp, with a large negative frequency component introduced at 60^o.

4 Discussion

The results obtained on the chirp are summarized in Table 1, where Δ chirp, the amplitude of the chirp is defined by the difference between the maximum and the minimum values of chirp. For no CW injection the chirp introduced by the SOA is very small, as negligible SPM occurs because the device is operating in the unsaturated regime. There is also a very small polarization dependence of less than 10 GHz between θ equal to 0^o and 60^o, may be due to the polarization dependence of the CH. The amplitude of the chirp increases with increase of CW injection. At 1 mW, a discrepancy between chirps at different value of $theta$ appears. For instance the value of Δ chirp at 0^o

or30^o is half of Δ chirp at 45^o or 60^o. This demonstrates the polarization dependence of carrier heating mechanism selected by the pulse width. This polarization dependence is even larger for 4 mW CW injection. A trend emerges from these results. Within the values of θ taken and the spectral resolution of the FROG, it is obvious that at 30^o the chirp remains minimum and that at 60^o is larger no matter what level of injection in CW is. The CW signal enhances the effect of the gain suppression and highlights the polarization dependence of the carrier-photon interaction. The FWM results (see Figs 3(a) and (b))showed also the same polarization dependence. Furthermore it was possible to discriminate the dependence of the CDP and CH, which is not possible with the FROG. At $\theta = 60^o$, the larger values for recovery time of CDP and CH were measured and at $\theta = 30^o$ the smallest values. These results indicate that 60^o is close to the TM axis of the device. For a tensile strained bulk device there are more TM transitions than TE transitions due to the shifting of the subbands in the valence band [17]. The light holes, which give rise to TM transitions are favored under such strain. A larger TM gain and so a greater depletion of carriers for injected light polarized along the TM axis are achieved. So TM light results in a lower carrier density population, this leads to a longer carrier recovery time due to the fact that the carrier lifetime is inversely proportional to carrier density. Due to the fact that the TM gain is higher than the TE gain in the tensile strained case, there would also be a larger shift towards lower wavelengths for the TM mode, as carriers in higher electron states would participate in the gain under such circumstances. As α_{cdp} is inversely proportional to the wavelength the result is that α_{cdp} would shift towards larger values for light polarized along the TM direction as observed in Fig. 3a).

There is no straight forward explanation for the dependance. We suggest that there is a modification of the eigen modes of the waveguide. As the

5 Conclusions

The polarization dependence of the gain dynamics in a bulk SOA have been measured using two independent experimental setups. Consistency was found between both setups. The first experimental setup measured the gain recovery time and LEF as a function of polarization using a CW FWM experiment, for both CDP and CH mechanisms. A polarization dependence of this effects has been demonstrated with a minimum receovery time at 30^0 and a maximum at 60^o. The second experimental setup measured the amplification of polarization resolved 2 ps pulses using the FROG technique. This technique allowed for the measurement of the pulses in both the temporal and spectral domains. Negligible polarization dependence was measured when the pulses were amplified in the linear gain regime of the device. However, when the gain of the device was saturated, a large polarization dependence was measured. The largest nonlinearity was measured for an injected polarization angle of 60^o. A chirp amplitude of 311 GHz was measured at 60^o for large gain suppression. A polarization dependence in the chirp amplitude of 143 GHz was measured under these conditions. The largest gain recovery time and LEF was measured at an angle of 60^o, in agreement with the FWM experiment performed in the first section. Both methods can be used to measure the polarization dependence of non-linear mechanism. This polarization dependence must be taken into account for SOA applications in optical networks, as depending on θ different recovery times can be achieved and different spectral components can be added to the transmittred signal.

6 Acknowledgement

This work is supported by Enterprise Ireland and the Science Foundation Ireland investigator programme.

References

[1] A. Poustie, Proc. ECOC 3 (2005) 475.

[2] P. Borri, S. Scaffetti, J. Mørk, W. Langbein, J.M. Hvam, A. Mecozzi, and F. Martelli, Opt. Commun. 164 (1999) 51.

[3] X. Yang, D. Lenstra, G.D. Khoe, and H.J.S. Dorren, Opt. Commun. 223 (2003) 169.

[4] Z. Li, X. Yang, E. Tangdiongga, H. Ju, G.D. Khoe, H.J.S. Dorren, and D. Lenstra, IEEE J. Quant. Electron. 41 (2005) 808.

[5] L.F. Tiemeijer, Appl. Phys. Lett. 59 (1991) 499.

[6] K. Kikuchi, M. Amano, C.E. Zah, and T.P. Lee, Appl. Phys. Lett. 64 (1994) 548.

[7] A. Mecozzi, Opt. Lett. 19 (1994) 892.

[8] S. Diez, C. Schimt, R. Ludwig, H.G. Weber, K. Obermann, S. Kindt, I. Koltchanov, and K. Petermann, IEEE J. Sel. Top. Quant. Electron. 3 (1997) 1131.

[9] S. Scotti, L. Graziani, A. D'Ottavi, F. Martelli, A. Mecozzi, P. Spano, R. Dall'Ara, F. Girandin, and G. Guekos, IEEE J. Sel. Top. in Quant. Electron. 3 (1997) 1156.

[10] S. Diez, C. Schimt, R. Ludwig, H.G. Weber, P. Doussiere, and T. Duceiller, IEEE Photon. Technol. Lett. 10 (1998) 212.

[11] K. Obermann, I. Koltchanov, K. Petermann, S. Diez, R. Ludwig, and H.G. Weber, IEEE J. Quant. Electron. 33 (1997) 81.

[12] G.P. Agrawal, and N. A. Olsson, IEEE J. Quant. Electron. 25 (1989) 2297.

[13] R. Trebino, K.W. Long, D.N. Fittinghoff, J.N. Sweetser, M.A. Krumbugel, and B.A. Richman, Rev. Sci. Ins. 68 (1997) 3277.

[14] H. Ghafouri-Shiraz, P.W. Tan, and T. Aruga, IEEE J. Sel. Top. in Quant. Electron. 3 (1997) 210.

[15] A.M. Clarke, M.J. Connelly, P. Anandarajah, L.P. Barry, and D. Reid, IEEE Photon. Technol. Lett. 17 (2005) 1800.

[16] A. Uskov, J. Mørk, and J. Mark, IEEE J. Quant. Electron. 30 (1994) 1769.

[17] E.P. O'Reilly, and A.R. Adams, IEEE J. Quant. Electron. 30 (1994) 366.